

Magnetic nanoparticles and ionic liquid effect on electrochemical sensor performance

Rudarsko-geološko-naftni zbornik
(The Mining-Geology-Petroleum Engineering Bulletin)
UDC: 622:669
DOI: 10.17794/rgn.2022.3.9

Original scientific paper



Farzaneh Shaker¹; Mohammad Taghi Vardini¹; Moosa Es'haghi¹; Ebrahim Ghorbani Kalhor¹

¹ Department of Chemistry, Tabriz Branch, Islamic Azad University, Tabriz, Iran.

Abstract

Magnetic nanoparticles and ionic liquid (IL, 1-hexyl-3-methyl-imidazolium bromide) based on graphene oxide (GO) composite provide unique physical and chemical properties in electrochemical sensor performance. Magnetic nanoparticles can cover active sites that increase chemical reactions with easy separation. IL increases the rate of electron transfer between the modified electrode and solution because it includes conductive adhesion properties. Also, IL in the next steps of design carbon paste electrodes (CPE) increases the cohesion. This study aims to investigate the effects of magnetic nanoparticles and IL on the electrochemical detection of dopamine (DA). DA has a vital role in the mammalian central nervous system and a change in its value from the standard range leads to a broad array of mental diseases. However, magnetic graphene oxide (MGO) may not be capable of enhancing electrochemical signs alone. In this regard, after the synthesis of MGO, IL was established on a composite. Then gold nanoparticles (AuNPs) and molecularly imprinted polymers (MIP) were modified into a MGO nanocomposite. MIP polymerization was continued by methacrylic acid (MAA) in the presence of DA as a template molecule. The developed sensor with modified nanocomposite was studied with cyclic voltammetry (CV) and differential pulse voltammetry (DPV) techniques. The modified sensor based on nanocomposite with a broad concentration linear range, between 1×10^{-7} to 1×10^{-4} mol L⁻¹ and a limit of detection of 1×10^{-8} mol L⁻¹ (S/N=3) was used for the detection of DA in biological samples. Furthermore, these results prove that MGO was improved on active sites of surface nanocomposite and IL increased conductivity in the based electrochemical sensor for DA detection.

Keywords:

magnetic nanoparticles; graphene oxide; ionic liquid; gold nanoparticles

1. Introduction

Graphene oxide (GO) composite is a carbon compound derived from the oxidation of graphite. The GO composite with high levels of oxygen functional groups and large surface areas as a novel carbon nanomaterial has an essential role in the electrochemical detection of biological compounds and metal heavy cations in real samples (Mengting et al., 2019) because oxygen functional groups and large surface areas increase the interaction between analyte molecules and composites.

Neurotransmitters are usually referred to as chemical compounds in the central nervous system that transmit messages between neurons (Si., Song, 2018). One of the critical neurotransmitters is dopamine (DA). DA plays an important role in motivational states and body movements. Therefore, changing the value of DA causes tremors and movement disorders (Briguglio et al., 2018).

The GO composite have various and excellent electrical and mechanical properties for biomedical applica-

tions but the modification of the GO surface is necessary for good results (Qureshi, Panesar, 2019). Magnetic nanoparticles based on GO composite have great advantages for magnetic separation in electrochemical and biomedical applications (Shahrebabak et al., 2019). These advantages include nanosize, a large specific surface area, paramagnetic, low toxicity, and biocompatible properties that make magnetic graphene oxide (MGO) nanocomposite remarkable in biosensors (Chou et al., 2019). However magnetic nanoparticles also can modify with different factors. One of the most important of them is ionic liquids.

Ionic liquids were used to develop the interaction mechanism between MGO-IL nanocomposite and analyte molecules (Alizadeh et al., 2020). Ionic liquids are composed of a cationic part and an anionic part. Ionic liquids due to special features such as high chemical, thermal stability, and high ionic conductivity improve the identification capacity of the nanocomposite. Also, the conductive adhesive property of ionic liquids increases cohesion in carbon paste electrodes (CPE) based on modified nanocomposite with magnetic nanoparticles (Gao et al., 2020). Ionic liquids create space between graphene layers and

Corresponding author: Mohammad Taghi Vardini
e-mail address: mtvardini@iaut.ac.ir

increase the specific surface area of nanocomposites because they decrease the aggregation of graphene (Chehreghani et al., 2021). As a result, the conductivity and electron transfer rate of the electrochemical system increase. However, step by step preparation time of MGO-IL nanocomposite may be long, so we have to be careful in setting the time (Qiu et al., 2020).

Gold nanoparticles (AuNPs) also were used as a complement factor in the conductivity of electrochemical sensors based on modified MGO-IL nanocomposite (Bolat, Abaci, 2018). The gold particles are very important because of their properties such as plasmon surface resonance, easy synthesis, various chemical surface modification methods, shape and size control, chemical inertness, and good biocompatibility (Theyagarajan et al., 2020). The addition of AuNPs into MGO-IL nanocomposite or modification of the MGO-IL nanocomposite surface by AuNPs develops the interaction of nanocomposite with target molecules by specific functional groups (Ye et al., 2021). Coating magnetite particles with AuNPs not only improves colloidal stability and the optical and conductive properties of magnetite particles, but also promotes their surface chemical reactions. In addition, it is possible to remotely control the locations with plasmonic properties using an external magnetic field (Jalilian et al., 2021).

The molecularly imprinted polymer (MIP) is another complementary factor in the designed nanocomposite that develops the CPE based on MGO-IL nanocomposite in the electrochemical system (Jalilian et al., 2021). Polymer nanocomposites have a high potential in electrochemical sensors because of their excellent advantages, such as good strength, large surface area to volume ratio, flexibility, and high selectivity. Therefore, these nanocomposites are successfully used in biomedical applications and biosensors (Zeb et al., 2021).

He et al. (2019) designed a novel MIP electrochemical sensor based on MnO_2 nanowires and reduced graphene oxide with good selectivity toward DA. Yu et al. (2012) fabricated a novel electrochemical sensor based on MIP, AuNPs, and SiO_2 composite for the determination of DA. Kan et al. (2012) prepared an electrochemical sensor based on a carbon nanotube/polypyrrole film for the determination of DA. These MIP sensors could be used for the electrochemical determination of DA, however, conductivity, and cohesion of MIP modified electrode is low because of the lack of magnetic graphene particles and IL in sensor structure.

In the current work, an MGO-IL-AuNPs-MIP nanocomposite was designed and used in an electrochemical system based on CPE to detect and determine DA in real samples. In this regard, after synthesis functionalized MGO-IL-AuNPs nanocomposite, MIP was synthesized chemically using functionalized MGO-IL-AuNPs nanocomposite, ethylene glycol dimethacrylate (EGDMA) as a cross-linker and methacrylic acid (MAA) as a functional monomer in the presence of DA as a template

molecule. The purpose of using the mentioned chemicals is the existence of oxygen and hydroxyl functional groups in the structure of chemicals. Since these functional groups developed electrochemical sensor performance by increasing the interactions of DA and modified nanocomposite. This modified nanocomposite is used to prepare CPE to measure DA. The MGO-IL-AuNPs-MIP nanocomposite was characterized by SEM and FT-IR methods. The CV, DPV, and electrochemical impedance spectroscopy (EIS) methods were employed to study the electrochemical behaviour of the fabricated sensor. To the best of the authors' knowledge, this is the first time that IL is grafted on the surface of MGO composite for the preparation of MIP nanocomposite. The prepared sensor showed high selectivity and sensitivity towards DA. After optimization, the designed sensor exhibited a wide linear range, a low detection limit, and an acceptable recovery for the determination of DA in real bio-samples.

2. Experimental

2.1. Chemicals

All the chemicals according to Table 1 were obtained with high laboratory grade almost close to more than 99% (Analytical chemistry grade).

2.2. Instruments of surface studying and electrochemical measurement

The morphology of the nanocomposite was investigated by Scanning Electron Microscope (SEM, S-2500, Hitachi High-tech International Trading Co., LTD, Shanghai, China) (accurate magnifier 10 to 100000 and accuracy of measurement: less than 5 to 10 μm). The structural properties of modified nanocomposite were studied by FT-IR spectra (JASCO FT/IR-6000 FTIR Spectrometer). Autolab PGSTAT302N (PGSTAT302N, Netherlands) was used for electrochemical measurements based on three electrodes that modified CPE with MGO and IL as the working electrode, platinum as the auxiliary electrode, and Ag/AgCl, KCl as the reference electrode. The modified CPE as the working electrode was immersed in the testing solution for 24 hours before use in the analysis. The EIS measurements were investigated by a $[\text{Fe}(\text{CN})_6]^{-3/-4}$ solution (wide frequency range: 100 kHz to 1 MHz; signal amplitude: 5 mV AC input). The Nyquist representation of the impedance data was analysed with the software ZSimpWin. The electrochemical performance of modified CPE was studied by CV and DPV techniques. These techniques were providing information about electrocatalytic reactions. The CV and DPV measurements are an investigation on current after applying a potential to the working electrode, but in CV measurement, potential increased with an increase in time, both in the direction of going and coming back. So, in the DPV technique, potential increased with an in-

Table 1: The properties of used chemicals

Chemicals	Company and country	Grade
Graphite powder in pure form and fine powder	Merck (Germany)	99% (Analytical chemistry grade)
Dopamine (DA)	Sigma Aldrich (USA)	99% (Analytical chemistry grade)
Ethylene glycol dimethacrylate (EGDMA)	Sigma Aldrich (USA)	99% (Analytical chemistry grade)
Methacrylic acid (MAA)	Merck (Germany)	99% (Analytical chemistry grade)
Azobisisobutyronitrile (AIBN)	Merck (Germany)	99% (Analytical chemistry grade)
IL; 1-hexyl-3-methyl-imidazolium bromide	Merck (Germany)	99% (Analytical chemistry grade)
Hydrochloric acid (HCl)	Merck (Germany)	99% (Analytical chemistry grade)
Sulphuric acid (H ₂ SO ₄)	Merck (Germany)	99% (Analytical chemistry grade)
Sodium nitrate (NaNO ₃)	Merck (Germany)	99% (Analytical chemistry grade)
Potassium permanganate (KMnO ₄)	Merck (Germany)	99% (Analytical chemistry grade)
Hydrogen peroxide (H ₂ O ₂)	Merck (Germany)	99% (Analytical chemistry grade)
Ferrous chloride (FeCl ₂)	Merck (Germany)	99% (Analytical chemistry grade)
Ferric chloride (FeCl ₃)	Merck (Germany)	99% (Analytical chemistry grade)
Chloroauric acid (HAuCl ₄)	Merck (Germany)	99% (Analytical chemistry grade)
Potassium ferricyanide K ₄ [Fe(CN) ₆]	Merck (Germany)	99% (Analytical chemistry grade)
Tri-sodium citrate	Merck (Germany)	99% (Analytical chemistry grade)
Potassium nitrate (KNO ₃)	Merck (Germany)	99% (Analytical chemistry grade)
Potassium chloride (KCl)	Merck (Germany)	99% (Analytical chemistry grade)
Sodium chloride (NaCl)	Merck (Germany)	99% (Analytical chemistry grade)
Potassium hydroxide (KOH)	Merck (Germany)	99% (Analytical chemistry grade)
Ammonium chloride (NH ₄ Cl)	Merck (Germany)	99% (Analytical chemistry grade)
Barium hydroxide (Ba(OH) ₂)	Merck (Germany)	99% (Analytical chemistry grade)
Zinc sulfate (ZnSO ₄)	Merck (Germany)	99% (Analytical chemistry grade)

crease in time in the pulsing form. These techniques were studied in the -2 to +2 potential range.

2.3. Synthesis of MGO-IL

Hummers' method was used for GO synthesis from fine and pure graphite powder (**Shahriary, Athawale, 2014**). For this purpose, a glass container was placed in an ice bath until the temperature reached under 10°C. Then 46 mL H₂SO₄, 2000 mg pure graphite powder, and 6000 mg KMnO₄ were stirred for 2 hours. The temperature was increased to 35°C in the bath. The resulting composition was diluted with 300 mL distilled water and H₂O₂ until the colour of the composition turned yellow. Then the pH of the resulting composition was increased while stirring for 1 hour until the solids of GO were deposited and dried. Magnetic particles were established on GO by mixing 350 mg FeCl₂, 500 mg FeCl₃, 50 mg of GO, and 100 mL distilled water under ultrasonic stirring for 30 minutes. The temperature and pH of the obtained mixture were positioned to 90°C and pH=9 respectively. The sediment particles after coated MGO were isolated in a magnet field and heated at 60°C under a vacuum oven. To prepare MGO-IL composite, 160 mg of magnetic particles and 37 mg of IL were added to 150 mL of distilled water and stirred at 50°C for 5 hours. After centrifugation and filtration, the remaining solids were washed with water and dried at 60°C for 24 hours.

2.4. Synthesis of AuNPs and MGO-IL-AuNPs-MIP

The gold solution was produced by a reduction in tri-sodium citrate by HAuCl₄ (**Yazdani et al., 2021**). Then, the suspension of AuNPs and MGO-IL particles were mixed mechanically for 2 hours until the solid particles were coated on the MGO-IL composite. Also, the MGO-IL-AuNPs-MIP nanocomposite was synthesized by chemical polymerization in a reflux system. The reflux system was heated for the chemical reaction for 24 hours, while the introduced vapour was cooled by a condenser. Therefore, 100 mg MGO-IL-AuNPs, 40 mL distilled water, 0.2 mmol DA, 0.4 mmol functional monomers, 4 mmol cross-linker, and 150 mg of the initiator were mixed, and it remained in the reflux system at 60°C for 24 hours. In the reflux system, the energy of the reaction between materials was increased and the rate of reaction also increased. The solid particles of MIP nanocomposite after synthesis and washing by acetonitrile separated based on magnetic properties. Template molecules were extracted from MIP composite by being placed in 50 mL of HCl solution (0.1 M) for 6 hours while stirring. The final product was dried at 60°C in a vacuum oven for 24 hours.

2.5. Preparation of CPE

The CPE compositions were composed with an optimum ratio of 100 mg synthesized nanocomposite, 40 mg

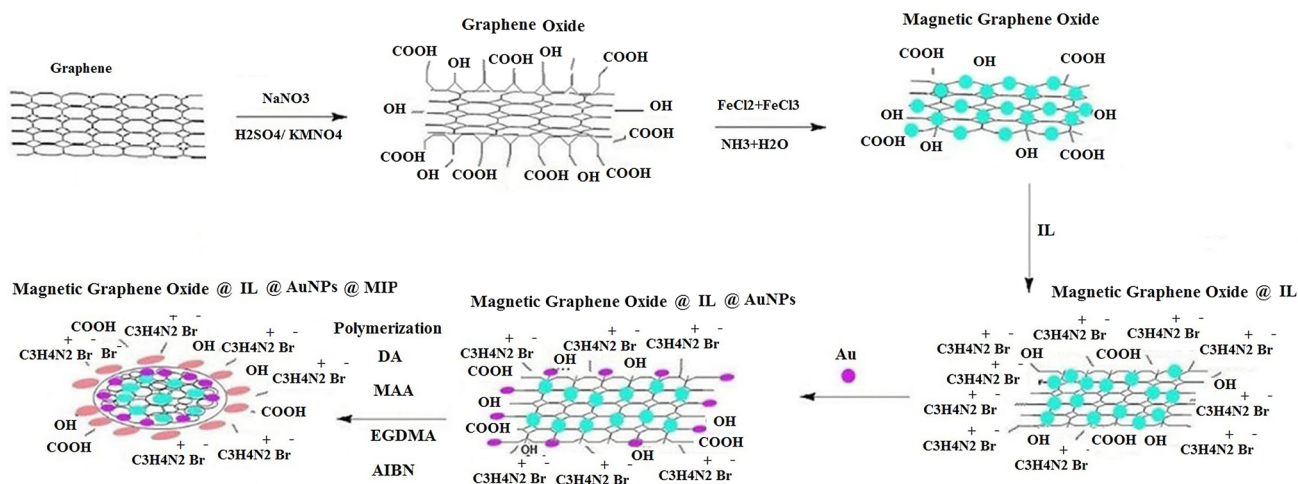


Figure 1: Preparation of MGO-IL-AuNPs-MIP nanocomposite by chemical polymerization of MIP

graphite, and 60 mg paraffin oil. The paraffin oil in the CPE structure was increased adhesion between graphite and modified nanocomposite. After complete formation of CPE by packing the CPE compositions in the narrow tubes and drying at laboratory temperature for 24 hours, the surface of the designed electrode (area of electrode: 4 mm) was smoothed by sandpaper and floated in acetonitrile solution as a supporting solution. As shown in **Figure 1**, stages of MGO-IL-AuNPs-MIP nanocomposite synthesis are depicted after preparation of MGO-IL-AuNPs nanocomposite, MIP polymerization developed by MAA, EGDMA, AIBN, and DA in an acetonitrile solution.

2.6. Preparation of urine and blood real samples

The performance of the proposed sensor in the detection of DA in the real samples was investigated by the preparation of samples. In this regard at first, the urine samples were centrifuged by adding 25 mL $\text{Ba}(\text{OH})_2$ (1 wt%) and 25 mL $1 \text{ mol L}^{-1} \text{ ZnSO}_4$ for 15 minutes at 2000 rpm. Then, the blood samples (1 mL blood serum + 1 mL acetonitrile) were centrifuged for 15 minutes at 180 rpm. In this way, proteins and molecules were deposited at the bottom of the test tubes and the samples were prepared. In the next stage, the applicable solution was prepared by adding concentrations of drug and prepared blood serum and urine samples with the addition of $0.1 \text{ mol L}^{-1} \text{ KNO}_3$.

3. Results and Discussion

3.1. Characterization

In the present study, coating properties of magnetic composite were described by SEM images. The FT-IR spectra were employed to characterize the structure of magnetic nanocomposite step by step. These studies to investigate magnetic particles and IL placed on polymeric nanocomposite were done.

The obtained images by SEM in **Figure 2** show different steps of the synthesized nanocomposite. The layers of GO are observed in **Figure 2a** with a sheet-wrinkles structures (Ahmad et al., 2018). The GO composite due to these creases has high surface areas and the contact level of the composite was increased. **Figure 2b** shows that the iron particles were dispersed on the GO plates irregularly. The MGO nanocomposite was constructed with relatively uniform porosity. **Figure 2c** shows the synthesized particles of MGO@IL (IL groups were coated on MGO). As can be noticed, the empty spaces of magnetic nanocomposite were somewhat filled by the IL cover.

The synthesized AuNPs are distributed over the surface composite regularly as shown in **Figure 2d**. The surface of MGO-IL nanocomposite was increased by covering with AuNPs. As a result, surface chemistry reactions were upgraded. **Figure 2e** shows the synthesized nanocomposite of MGO-IL-AuNPs-MIP. The wrinkles are not observable in **Figure 2e** because all particles are covered by polymer layers. These results prove that according to earlier researchers' studies, GO creases are gradually lowered by the placement of MGO-IL-AuNPs and MIP layers on the composite (Dramou et al., 2022). So, with this process, particle size and the detection power of nanocomposites increased according to discussions.

The FT-IR spectrum was examined according to **Figure 3**. The FT-IR spectrum in **Figure 3** (curve a) shows GO composite which confirmed oxidation graphite that created the C–O bond at 1178 cm^{-1} . The absorption band in 1626 cm^{-1} is related to the unoxidized graphite that compared the previous band is wider and shows a C–C bond in graphite layers. The FT-IR spectrum in **Figure 3** (curve b) shows a strong absorption band in 571 cm^{-1} and is interconnected to the magnetic Fe–O bond that proves the magnetization of GO.

The FT-IR spectrum in **Figure 3** (curve c) has an absorption band in 1094 cm^{-1} that is related to the IL connection. Furthermore, as shown in **Figure 3** (curve d) the FT-

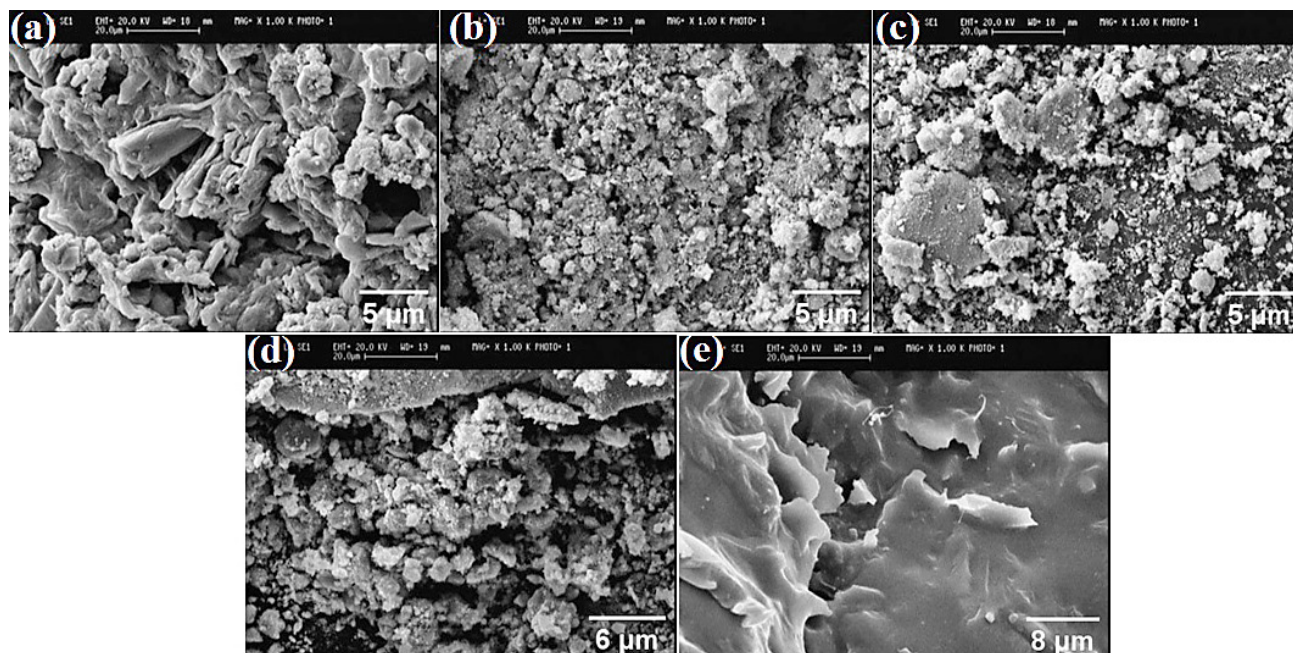


Figure 2: SEM images of GO (a), MGO (b), MGO@IL (c), MGO@IL-AuNPs (d), and MGO-IL-AuNPs-MIP (e)

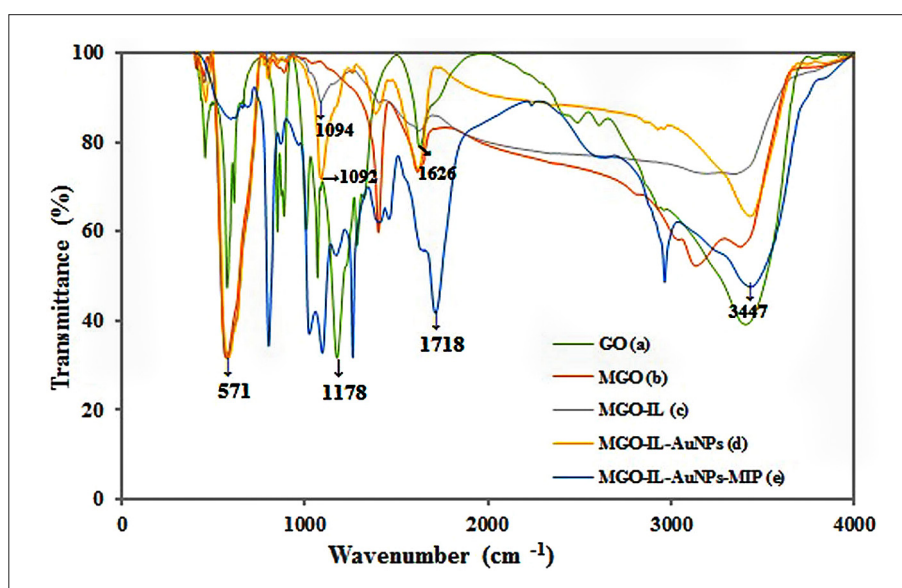


Figure 3: The FT-IR spectra of GO (a), MGO (b), MGO-IL(c), MGO-IL-AuNPs (d), and MGO-IL-AuNPs-MIP (e) for investigating MGO-IL-AuNPs-MIP nanocomposite structure

IR spectrum of MGO-IL-AuNPs exhibited a sharp absorption band compared to the previous step at 1092 cm⁻¹, which revealed the connection of AuNPs on the MGO-IL composite surface through covalent bonding. Finally, as shown in Figure 3 (curve e) the strong absorption band at 1718 cm⁻¹ was related to the carbonyl group, and the weak absorption band at 3447 cm⁻¹ was due to the O-H group in the MIP layer. Therefore, the FT-IR spectra confirmed that magnetic particles besides IL, AuNPs, and MIP are cited on nanocomposite. In this process, areas with a very specific molecular arrangement were formed in a polymer matrix according to previous studies and increased the

interaction between nanocomposite and target molecules (Dramou et al., 2019).

3.2. Effect of MGO and IL on the electrochemical and voltammetry behaviour of the electrode

In order to investigate the effect of modifying materials such as MGO and IL on the electrochemical behaviour of the proposed electrode, various modified electrodes were studied by the EIS method.

The EIS data were studied according to Figure 4 (chart A) using the curve of the bare electrode (pure

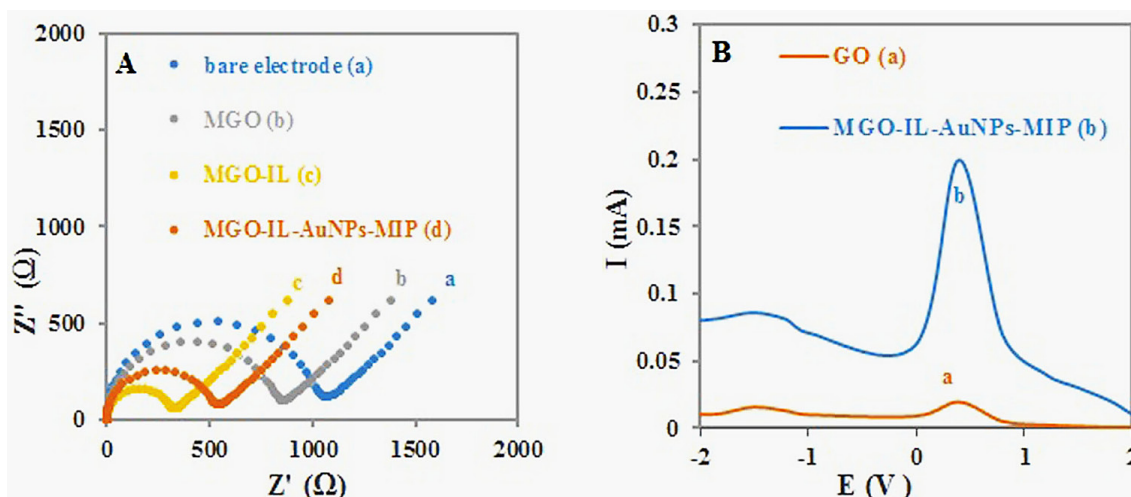


Figure 4: Chart A: Impedance spectra in a $0.02 \text{ mol L}^{-1} [\text{Fe}(\text{CN})_6]^{-3/-4}$ solution: bare electrode (curve a), MGO electrode (curve b), MGO-IL electrode (curve c), and of MGO-IL-AuNPs-MIP electrode (curve d) for investigating the effect of adding MGO and IL on the electrochemical behaviour. Chart B: The DPV spectra in a $10^{-4} \text{ mol L}^{-1}$ DA: GO (a) and MGO-IL-AuNPs-MIP (b) electrodes for investigating the effect of adding MGO and IL on the voltammetry behaviour

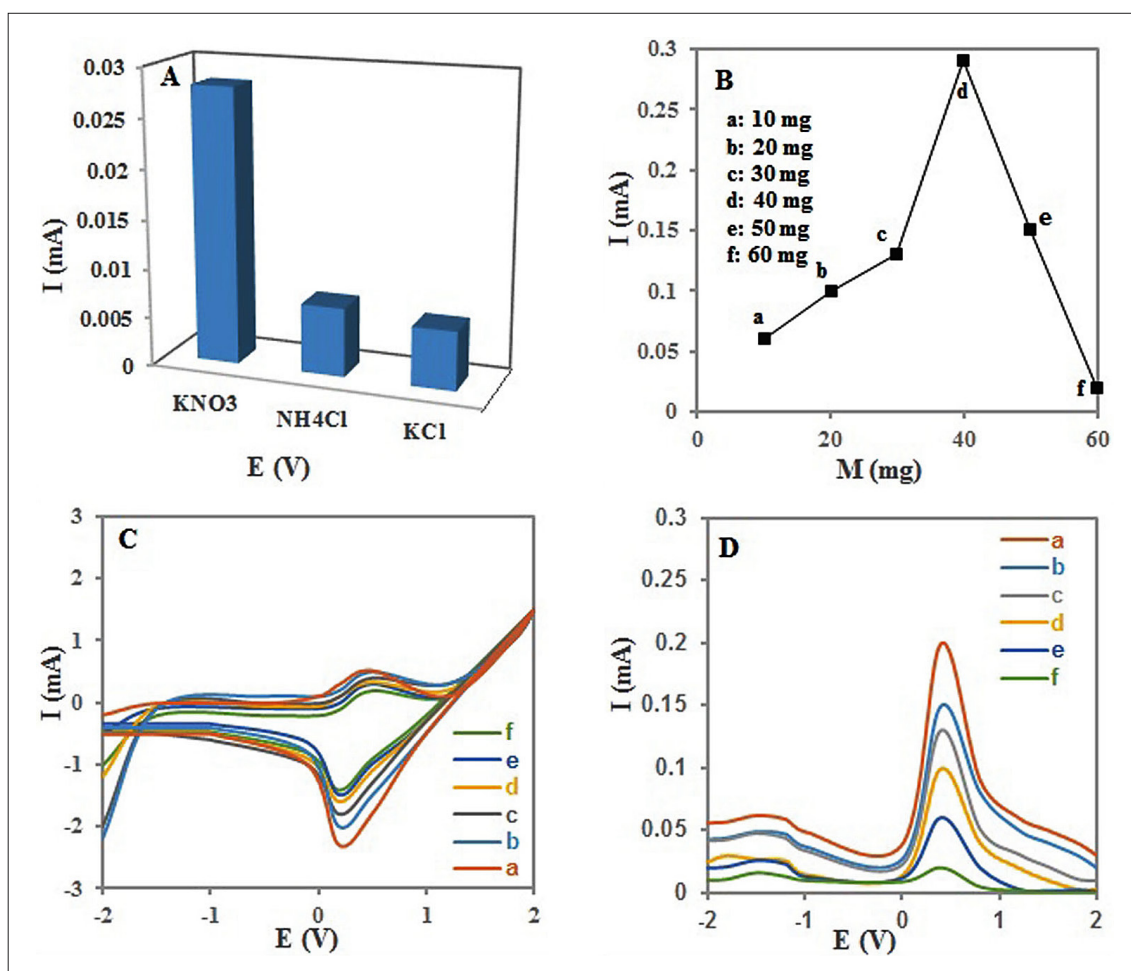


Figure 5: Chart A: Optimization of supporting electrolyte in $10^{-4} \text{ mol L}^{-1}$ DA (pH=7). Chart B: The effect of the amount of the nanocomposite with different amounts of nanocomposite, respectively on the modified electrode (a: 10 mg, b: 20 mg, c: 30 mg, d: 40 mg, e: 50 mg, and f: 60 mg). Chart C, D: The CV and DPV spectra of the modified electrode in the different DA solution with 40 mg amount of MGO-IL-AuNPs-MIP on the CPE (a: 10^{-4} , b: 10^{-5} , c: 2×10^{-5} , d: 4×10^{-5} , e: 6×10^{-5} and f: $8 \times 10^{-5} \text{ mol L}^{-1}$ DA) (pH=7; the scan rate= 0.1 V s^{-1})

graphite electrode) (curve a), MGO electrode (curve b), MGO-IL electrode (curve c), and of MGO-IL-AuNPs-MIP electrode (curve d) in $0.02 \text{ mol L}^{-1} [\text{Fe}(\text{CN})_6]^{3-/4-}$ solution in high frequency. The obtained results of **Figure 4** (chart A) indicate the Nyquist plot lines (**Gomes Jr et al., 2018**). It means with the increasing diameter of EIS diagrams (semicircle) the charge transfer resistance (R_{ct}) was increased. According to **Figure 4** (chart A), the diameter of the EIS diagrams and R_{ct} decreased with the addition of magnetic nanoparticles (curve b) and IL (curve c) in electrodes compared to the bare (pure graphite) electrode (curve a). However, after the addition of gold and MIP particles to the modified electrode, the diameter of EIS diagrams and R_{ct} of the MGO-IL-AuNPs-MIP electrode increased compared to MGO-IL because the MIP particles blocked the electron exchange between the solution and the electrode (curve d). The results confirmed the electrodes modified MGO and IL nanocomposite, and according to previous studies, increased the conductivity of the modified electrodes (**Mariappan et al., 2021**). The electroactive surface area of the modified electrode with the addition of MGO nanoparticles was increased. The stability and conductivity of the proposed electrode were developed by IL. Also, an electrocatalyst was developed by MGO and IL beside AuNPs. Finally, all these factors increased the electron exchange between the solution and the proposed electrode.

The voltammetry behaviour of the proposed electrode was studied by DPV and the effect of adding MGO and IL on the peak current became clear. To interpret the roles of MGO nanoparticles and IL of the proposed electrode, the DPV curves of the GO and MGO-IL-AuNPs-MIP electrodes were compared in the DA solution ($10^{-4} \text{ mol L}^{-1}$). As shown in **Figure 4** (chart B), the DPV of the MGO-IL-AuNPs-MIP electrode showed an apparent peak with high intensity at the potential of 0.19 V (curve a). The MGO nanoparticles enhanced the surface area of the electrode and had a better electrocatalytic activity for DA. When the IL was coated on the MGO composite beside MGO, the effect of gold nanoparticles was increased. Finally, electron transferability was increased and in turn enhanced the current in the proposed electrode based on modified polymeric nanocomposite (curve b).

3.3. Effect of the amount of MGO-IL-AuNPs-MIP nanocomposite on the electrode response

The effect of the amount of MGO-IL-AuNPs-MIP on DA peak current after optimization of the supporting electrolyte and pH was studied by CV and DPV methods. For this purpose, firstly the supporting electrolyte and pH were optimized. According to the results in **Figure 5** (chart A), the $0.1 \text{ mol L}^{-1} \text{KNO}_3$ solution at pH=7 was selected as the optimum supporting electrolyte in the analysis solution. The peak current in 0.1 M KNO_3 solution at pH=7 was high because by adding 0.1 mol L

$^{-1} \text{KNO}_3$ solution at pH=7 in studying solution, conductivity was increased. Secondly, the amount of MGO-IL-AuNPs-MIP on the CPE structure was optimized. Based on the results of **Figure 5** (chart B), the peak current was increased when the amount of the MGO-IL polymeric nanocomposite increased toward 40 mg . The best peak current was observed in the DA solution when the amount of the MGO-IL polymeric nanocomposite was close to 40 mg . However, when the amount of the MGO-IL polymeric nanocomposite was more than 40 mg , the current decreased dramatically because changing the MGO-IL polymeric nanocomposite from 40 mg leads to the inflation and destruction of the available binding sites of CPE structure (**Yang et al., 2019**). The peak current of DA as shown in **Figure 5** (chart C, D) was studied in the different DA solutions with 40 mg amount of MGO-IL-AuNPs-MIP on the CPE in CV and DPV spectra. As a result, 40 mg of MGO-IL-AuNPs-MIP nanocomposite was used in the CPE structure as a working electrode in the electrochemical system for DA measurement in biological samples.

3.4. Effect of the influence of scan rate on the MGO-IL modified electrode response

Scan rate is an important parameter for a better understanding of the electrochemical system. Various scan rates were investigated on the electrochemical behaviour of DA in pH=7 from -2 to 2 V by CV spectra. According to **Figure 6** (chart A) the redox peak current of DA was increased linearly with increasing scan rate (0.025 to 0.1 V s^{-1}).

Thus, it can be concluded that increasing the scan rate had an optimal effect on DA peak current. The regression equation as shown in **Figure 6** (chart B) was: (**Equation 1**)

$$\begin{aligned} I_{pa} \text{ (A)} &= 0.00196 v + 0.021, (R^2 = 0.978); \\ I_{pc} \text{ (A)} &= -0.0008 v - 0.00121, (R^2 = 0.9823) \end{aligned} \quad (1)$$

The R^2 Symbol in the equation is the coefficient of determination) for anodic and cathodic peaks, respectively. These equations confirmed that the redox of DA was controlled by the diffusion process. Moreover, the peak potential as shown in **Figure 6** (chart C) (E_p) increased linearly with logarithm of the scan rate ($\log v$) (0.025 to 0.1 V s^{-1}). The regression equation was: (**Equation 2**)

$$\begin{aligned} E_{pa} \text{ (V)} &= 0.7761 \log v + 1.7065, (R^2 = 0.9136); \\ E_{pc} \text{ (V)} &= -0.1818 \log v - 0.1051, (R^2 = 0.9831) \end{aligned} \quad (2)$$

The results indicated the electrochemical process according to Lavrion's equation was a quasi-reversible reaction (**Chukanov et al., 2018**). As shown in **Figure 6** (chart D) linear relationship between peak potentials (E_p) and pH was: (**Equation 3**)

$$\begin{aligned} E_{pa} &= 0.0604 \text{ pH} + 0.0168, (R^2=0.08957); \\ E_{pc} &= -0.0697 \text{ pH} + 0.0988, (R^2 = 0.9051) \end{aligned} \quad (3)$$

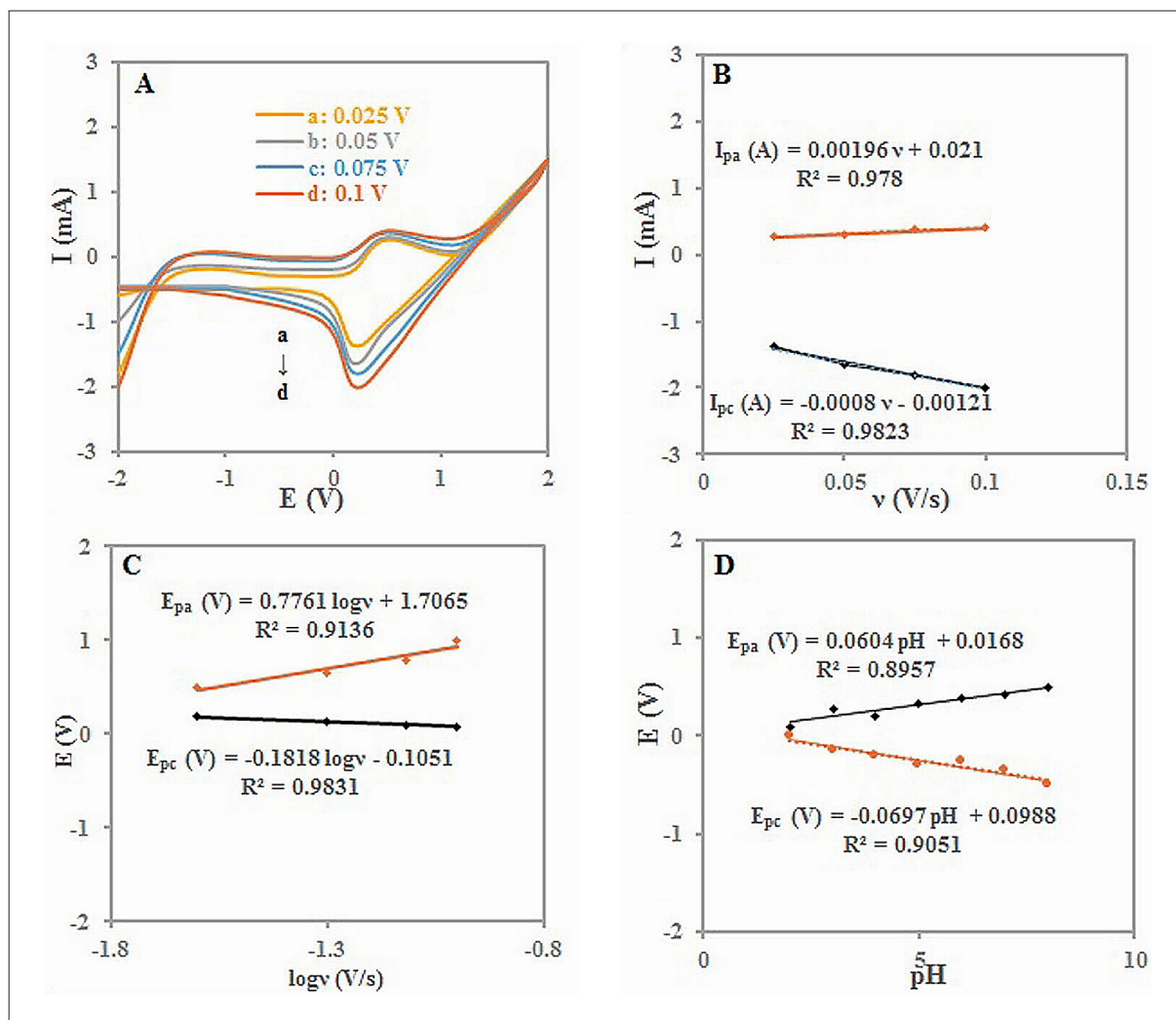


Figure 6: Chart A: The CV spectrums of the 10^{-4} mol L $^{-1}$ DA solution at different scan rates of 0.025; 0.05; 0.075; and 0.1 V s $^{-1}$ (d) (pH=7). Chart B: The anodic and cathodic peak currents of 10^{-4} mol L $^{-1}$ DA solution at different scan rates of 0.025, 0.05, 0.075, 0.1 V s $^{-1}$. Chart C: The anodic and cathodic peak potentials of DA at different logarithm scan rates of 0.025, 0.05, 0.075, 0.1 V s $^{-1}$. Chart D: The anodic and cathodic peak potentials of 10^{-4} mol L $^{-1}$ DA solution with a scan rate of 0.1 V s $^{-1}$ at different pH of 2, 3, 4, 5, 6, 7, 8

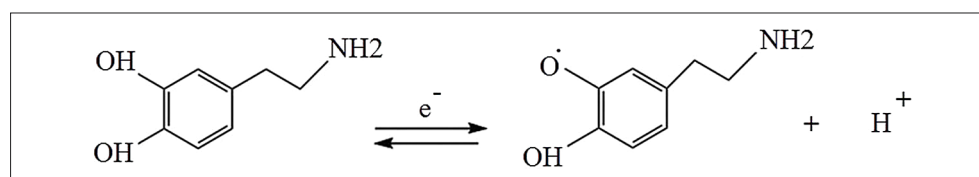


Figure 7: The electrochemical mechanism of DA at the electrode modified with MGO-IL-AuNPs-MIP

The slopes (0.0604 and 0.0697 V/pH) were closed to 0.059 V/pH, indicating that the number of protons transferred is equal to the electron (Palakollu, Karpoornath, 2018). The exchange $1e^-$, $1H^+$ of DA mechanism, herein, was proposed for DA electrochemical mechanism conforming **Figure 7**.

3.5. Analytical properties of the modified electrode

The analytical properties of the electrode modified with MGO-IL-AuNPs-MIP nanocomposite were investigated

by calibration curve and application of proposed electrode for DA detection in biological samples. Firstly, the calibration curve of DA was studied by DPV spectra as the optimum method to detect low values of DA at different concentrations of DA. The DPV spectra of different concentrations of DA are illustrated in **Figure 8** (Chart A).

Under optimal conditions, as shown in **Figure 8** (chart B) the linear concentration range was 1×10^{-7} to 1×10^{-4} mol L $^{-1}$ DA. The regression equation was: (**Equation 4**)

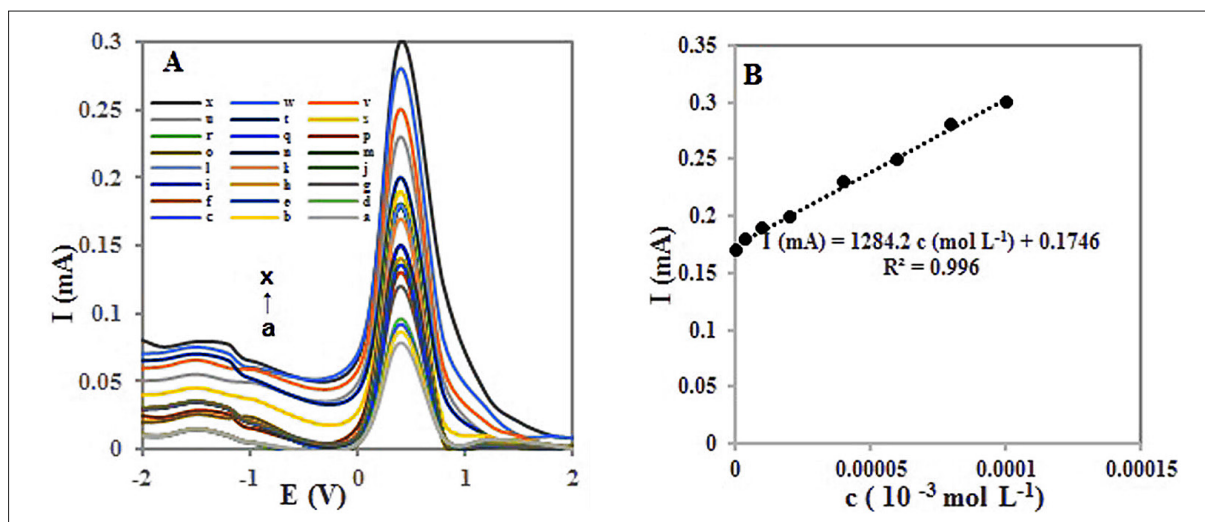


Figure 8: Chart A: The DPV spectra of 1×10^{-8} , 2×10^{-8} , 4×10^{-8} , 6×10^{-8} , 8×10^{-8} , 1×10^{-7} , 2×10^{-7} , 4×10^{-7} , 7×10^{-7} , 1×10^{-6} , 2×10^{-6} , 4×10^{-6} , 8×10^{-6} , 1×10^{-5} , 2×10^{-5} , 4×10^{-5} , 6×10^{-5} , 8×10^{-5} , 1×10^{-4} , 2×10^{-4} , 4×10^{-4} , 6×10^{-4} , 8×10^{-4} , and 1×10^{-3} mol L⁻¹ DA solutions (pH=7; scan rate=0.1 V s⁻¹). Chart B: The linear relationship between the electrochemical signal and the concentration of DA (the concentrations of DA were: 1×10^{-7} , 4×10^{-7} , 1×10^{-5} , 2×10^{-5} , 4×10^{-5} , 6×10^{-5} , 8×10^{-5} , and 1×10^{-4} mol L⁻¹)

Table 2: The analytical properties of different detection methods for the determination of DA

Procedure	Detection limit / mol L ⁻¹	Linear range / mol L ⁻¹	References
CV as electrochemical method by a modified glassy electrode	3×10^{-7}	2×10^{-6} to 8×10^{-5}	(Dramou et al., 2019)
CV as electrochemical method by a modified gold electrode	8×10^{-7}	1×10^{-6} to 2×10^{-4}	(Liu et al., 2004)
CV as electrochemical method by a carbon nanotubes-ionic liquid gel modified electrode	1×10^{-7}	1×10^{-6} to 1×10^{-4}	(Zhao et al., 2005)
Electrochemical procedure based on nitrogen doped graphene: Simultaneous	2.5×10^{-7}	5×10^{-7} to 1.7×10^{-4}	(Sheng et al., 2012)
MGO-IL-Au NPs-MIP nanocomposite	1×10^{-8}	1×10^{-7} to 1×10^{-4}	This work

$$I(\text{mA}) = 1284.2 c (\text{mol L}^{-1}) + 0.1746 (R^2 = 0.996) \quad (4)$$

The detection limit was estimated to be 1×10^{-8} mol L⁻¹ (S/N=3). The S/N symbol is the Signal to Noise ratio that the peak current is the real signal in this electrochemical system. According to the results obtained from the calibration curve and **Table 2** data, the MGO-IL-

Table 3: The determination of DA in real samples (n=3)

Samples	Added (10^{-3} mol L ⁻¹)	Found (10^{-3} mol L ⁻¹)	Recovery (%)	RSD (%)
Urine	1.5	1.48	98	2.2
	3.1	3.09	99.66	1.4
	4.5	4.48	99.5	1.7
Blood	1	1.01	100>	2
	3.3	3.29	99.69	1.3

AuNPs- MIP modified electrode in comparison with other electrochemical methods has a wide concentration range and low detection limit. These results indicate a good and positive effect of magnetic and IL nanocomposite on electrode performance. Therefore, the rate of electron transfers and conductivity of the modified electrode with MGO-IL-AuNPs-MIP nanocomposite were increased due to the unique conduction properties of MGO and IL nanocomposite.

To assess the applicability and reliability of the modified electrode with MGO-IL-AuNPs- MIP nanocomposite, DA was determined for blood serum and urine samples using standard addition procedure. In the standard addition procedure, the matrix of applicable blood and urine solutions is the same, often by adding the specific concentrations of drug solution. The applicable solution was analysed by DPV spectra. The modified electrode with MGO-IL-AuNPs-MIP nanocomposite had selectivity towards the DA template molecules. The recovery percentage and the Relative Standard Deviation (RSD) of the proposed electrode are presented in **Table 3**. Good measurement accuracy was obtained and the recovery range was 98%> (for every three repetitions of each applied sample). If additional values of DA solution in the

applied samples are appropriate, recovery percentage and RSD also is in good range because the error rate is reduced. These results suggest that the proposed electrode can be used to analyse DA in real samples. Determination of DA as critical neurotransmitters in the human body is essential, therefore the proposed electrode was used as an applied method in the biomedical area.

All experimental procedures were accomplished in the laboratory of the Islamic Azad University of Tabriz and agreement with Guidelines IR.IAU.REC (Ethics Committee of Islamic Azad University). The research was completed by contributors with personal satisfaction before sampling them (blood and urine samples).

4. Conclusions

In this work, the effect of magnetic nanoparticles and ionic liquid on electrochemical sensor performance for DA detection in real samples was studied. Magnetic nanoparticles and ionic liquid create a new electrochemical platform in the biomedical area by developing the detection ability of electrochemical sensors. Magnetic nanoparticles increased conductivity and surface area for the reaction of nanocomposite based on an electrochemical sensor. Also, magnetic nanoparticles increased stability by decreasing the toxic properties of test background, drugs, and chemicals. The ionic liquid increased the adhesion property of the nanocomposite and the conductivity of the electrochemical sensor was modified by the designed nanocomposite. Eventually, ionic liquid and magnetic particles increased the cohesion in the CPE structure. Also, AuNPs and MIP particles beside magnetic nanoparticles and ionic liquid increased electrocatalytic activity and the stability of the proposed sensor. As a result, the designed sensor was used as an effective electrochemical sensor in the detection of DA in bio-real samples.

5. References

- Ahmad, H., Fan, M., Hui, D. (2018): Graphene oxide incorporated functional materials: A review. *Composites Part B: Engineering*, 145, 270-280. <https://doi.org/10.1016/j.compositesb.2018.02.006>.
- Alizadeh, M., Azar, P. A., Mozaffari, S. A., Karimi-Maleh, H., Tamaddon, A.-M. (2020): A DNA based biosensor amplified with ZIF-8/ionic liquid composite for determination of mitoxantrone anticancer drug: an experimental/docking investigation. *Frontiers in Chemistry*, 8, 814. <https://doi.org/10.3389/fchem.2020.00814>.
- Bolat, G., Abaci, S. (2018): Non-enzymatic electrochemical sensing of malathion pesticide in tomato and apple samples based on gold nanoparticles-chitosan-ionic liquid hybrid nanocomposite. *Sensors*, 3, 18, 773. <https://doi.org/10.3390/s18030773>.
- Briguglio, M., Dell'Osso, B., Panzica, G., Malgaroli, A., Banfi, G., Zanaboni Dina, C., Galentino, R., Porta, M. (2018): Dietary neurotransmitters: a narrative review on current knowledge. *Nutrients*, 5, 10, 591. <https://doi.org/10.3390/nu10050591>.
- Chehrehgani, S., Yari, M., Zeynali, A., Akhgar, B. N., Gharagheshlagh, H. H., Pishravian, M. (2021): Optimization of Chalcopyrite Galvanic Leaching in the Presence of Pyrite and Silver as Catalysts by using Response Surface Methodology (RSM). *Rudarsko-geološko-naftni zbornik*, 1, 36, 37-47. <https://doi.org/10.17794/rgn.2021.1.4>.
- Chou, J.-C., Wu, C.-Y., Kuo, P.-Y., Lai, C.-H., Nien, Y.-H., Wu, Y.-X., Lin, S.-H., Liao, Y.-H. (2019): The flexible urea biosensor using magnetic nanoparticles. *IEEE Transactions on Nanotechnology*, 18, 484-490. <https://doi.org/10.1109/TNANO.2019.2895137>.
- Chukanov, N. V., Pekov, I. V., Belakovskiy, D. I., Britvin, S. N., Stergiou, V., Voudouris, P., Magganas, A. (2018): Katerinopoulosite, (NH₄)₂Zn(SO₄)₂·6H₂O, a new mineral from the Esperanza mine, Lavrion, Greece. *European Journal of Mineralogy*, 4, 30, 821-826. <https://doi.org/10.1127/ejm/2018/0030-2746>.
- Dramou, P., Itatahine, A., Fizir, M., Mehdi, Y. A., Kutoka, P. T., He, H. (2019): Preparation of novel molecularly imprinted magnetic graphene oxide and their application for quercetin determination. *Journal of Chromatography B*, 1124, 273-283. <https://doi.org/10.1016/j.jchromb.2019.06.007>.
- Dramou, P., Wang, F., Sun, Y., Zhang, J., Yang, P., Liu, D., He, H. (2022): Synthesis and characterization of superparamagnetic graphene oxide assembled halloysite composites for extraction of rutin. *Applied Clay Science*, 217, 106397. <https://doi.org/10.1016/j.clay.2021.106397>.
- Gao, Z., Kong, L., Jin, R., Liu, X., Hu, W., Gao, G. (2020): Mechanical, adhesive and self-healing ionic liquid hydrogels for electrolytes and flexible strain sensors. *Journal of Materials Chemistry C*, 32, 8, 11119-11127.
- Gomes Jr, S., Guimarães, C., Martins, N., Taranto, G. (2018): Damped Nyquist Plot for a pole placement design of power system stabilizers. *Electric Power Systems Research*, 158, 158-169. <https://doi.org/10.1016/j.epsr.2018.01.012>.
- He, Q., Liu, J., Liu, X., Li, G., Chen, D., Deng, P., Liang, J. (2019): A promising sensing platform toward dopamine using MnO₂ nanowires/electro-reduced graphene oxide composites. *Electrochimica Acta*, 296, 683-692. <https://doi.org/10.1016/j.electacta.2018.11.096>.
- Jalilian, R., Ezzatzadeh, E., Taheri, A. (2021): A novel self-assembled gold nanoparticles-molecularly imprinted modified carbon ionic liquid electrode with high sensitivity and selectivity for the rapid determination of bisphenol A leached from plastic containers. *Journal of Environmental Chemical Engineering*, 4, 9, 105513. <https://doi.org/10.1016/j.jece.2021.105513>.
- Kan, X., Zhou, H., Li, C., Zhu, A., Xing, Z., Zhao, Z. (2012): Imprinted electrochemical sensor for dopamine recognition and determination based on a carbon nanotube/polypyrrole film. *Electrochimica Acta*, 63, 69-75. <https://doi.org/10.1016/j.electacta.2011.12.086>.
- Liu, T., Li, M., Li, Q. (2004): Electroanalysis of dopamine at a gold electrode modified with N-acetylcysteine self-assem-

- bled monolayer. *Talanta*, 4, 63, 1053-1059. <https://doi.org/10.1016/j.talanta.2004.01.019>.
- Mariappan, V. K., Krishnamoorthy, K., Manoharan, S., Pazhamalai, P., Kim, S. J. (2021): Electrospun Polymer-Derived Carbyne Supercapacitor for Alternating Current Line Filtering. *Small*, 34, 17, 2102971. <https://doi.org/10.1002/sml.202102971>.
- Mengting, Z., Kurniawan, T. A., Fei, S., Ouyang, T., Othman, M. H. D., Rezakazemi, M., Shirazian, S. (2019): Applicability of BaTiO₃/graphene oxide (GO) composite for enhanced photodegradation of methylene blue (MB) in synthetic wastewater under UV-vis irradiation. *Environmental Pollution*, 255, 113182. <https://doi.org/10.1016/j.envpol.2019.113182>.
- Palakollu, V. N., Karpoomath, R. (2018): Enhanced electrochemical sensing of dopamine based on carboxylic acid functionalized multi-walled carbon nanotubes/poly (toluidine blue) composite. *Synthetic Metals*, 245, 87-95. <https://doi.org/10.1016/j.synthmet.2018.08.012>.
- Qiu, X., Wang, Y., Xue, Y., Li, W., Hu, Y. (2020): Laccase immobilized on magnetic nanoparticles modified by amino-functionalized ionic liquid via dialdehyde starch for phenolic compounds biodegradation. *Chemical Engineering Journal*, 391, 123564. <https://doi.org/10.1016/j.cej.2019.123564>.
- Qureshi, T. S., Panesar, D. K. (2019): Impact of graphene oxide and highly reduced graphene oxide on cement based composites. *Construction and Building Materials*, 206, 71-83. <https://doi.org/10.1016/j.conbuildmat.2019.01.176>.
- Shahrehabak, S. M., Saber-Tehrani, M., Faraji, M., Shabaniyan, M., Aberoomand-Azar, P. (2019): Simultaneous magnetic solid phase extraction of acidic and basic pesticides using triazine-based polymeric network modified magnetic nanoparticles/graphene oxide nanocomposite in water and food samples. *Microchemical Journal*, 146, 630-639. <https://doi.org/10.1016/j.microc.2019.01.047>.
- Shahriary, L., Athawale, A. A. (2014): Graphene oxide synthesized by using modified hummers approach. *Int. J. Renew. Energy Environ. Eng.*, 01, 2, 58-63.
- Sheng, Z.-H., Zheng, X.-Q., Xu, J.-Y., Bao, W.-J., Wang, F.-B., Xia, X.-H. (2012): Electrochemical sensor based on nitrogen doped graphene: simultaneous determination of ascorbic acid, dopamine and uric acid. *Biosensors and Bioelectronics*, 1, 34, 125-131. <https://doi.org/10.1016/j.bios.2012.01.030>.
- Si, B., Song, E. (2018): Recent advances in the detection of neurotransmitters. *Chemosensors*, 1, 6, 1. <https://doi.org/10.3390/chemosensors6010001>.
- Theyagarajan, K., Yadav, S., Satija, J., Thenmozhi, K., Senthilkumar, S. (2020): Gold nanoparticle-redox ionic liquid based nanoconjugated matrix as a novel multifunctional biosensing interface. *ACS Biomaterials Science & Engineering*, 11, 6, 6076-6085. <https://doi.org/10.1021/acsbio-materials.0c00807>.
- Yang, C., Zhang, C., Huang, T., Dong, X., Hua, L. (2019): Ultra-long ZnO/carbon nanofiber as free-standing electrochemical sensor for dopamine in the presence of uric acid. *Journal of Materials Science*, 24, 54, 14897-14904. <https://doi.org/10.1007/s10853-019-04000-x>.
- Yazdani, S., Daneshkhah, A., Diwate, A., Patel, H., Smith, J., Reul, O., Cheng, R., Izadian, A., Hajrasouliha, A. R. (2021): Model for gold nanoparticle synthesis: Effect of pH and reaction time. *ACS omega*, 26, 6, 16847-16853. <https://doi.org/10.1021/acsomega.1c01418>.
- Ye, C., Chen, X., Zhang, D., Xu, J., Xi, H., Wu, T., Deng, D., Xiong, C., Zhang, J., Huang, G. (2021): Study on the properties and reaction mechanism of polypyrrole@ norfloxacin molecularly imprinted electrochemical sensor based on three-dimensional CoFe-MOFs/AuNPs. *Electrochimica Acta*, 379, 138174. <https://doi.org/10.1016/j.electacta.2021.138174>.
- Yu, D., Zeng, Y., Qi, Y., Zhou, T., Shi, G. (2012): A novel electrochemical sensor for determination of dopamine based on AuNPs@ SiO₂ core-shell imprinted composite. *Biosensors and Bioelectronics*, 1, 38, 270-277. <https://doi.org/10.1016/j.bios.2012.05.045>.
- Zeb, S., Wong, A., Khan, S., Hussain, S., Sotomayor, M. D. (2021): Using magnetic nanoparticles/MIP-based electrochemical sensor for quantification of tetracycline in milk samples. *Journal of Electroanalytical Chemistry*, 900, 115713. <https://doi.org/10.1016/j.jelechem.2021.115713>.
- Zhao, Y., Gao, Y., Zhan, D., Liu, H., Zhao, Q., Kou, Y., Shao, Y., Li, M., Zhuang, Q., Zhu, Z. (2005): Selective detection of dopamine in the presence of ascorbic acid and uric acid by a carbon nanotubes-ionic liquid gel modified electrode. *Talanta*, 1, 66, 51-57. <https://doi.org/10.1016/j.talanta.2004.09.019>.

SAŽETAK

Učinak magnetnih nanočestica i ionske tekućine na performanse elektrokemijskih senzora

Magnetne nanočestice i ionska tekućina (IL, 1-heksil-3-metil-imidazolijev bromid) na bazi kompozita grafenova oksida (GO) pružaju jedinstvena fizička i kemijska svojstva u izvedbi elektrokemijskih senzora. Magnetne nanočestice mogu pokriti aktivna mjesta koja povećavaju kemijske reakcije uz jednostavno odvajanje. IL povećava brzinu prijenosa elektrona između modificirane elektrode i otopine jer uključuje svojstva vodljive adhezije. Također, IL u sljedećim koracima dizajna elektroda ugljične paste (CPE) povećava koheziju. Cilj je studije proučavanje učinaka magnetnih nanočestica i IL-a na elektrokemijsku detekciju dopamina (DA). DA ima vitalnu ulogu u središnjemu živčanom sustavu sisavaca i promjena njegove vrijednosti iz standardnoga raspona dovodi do širokoga raspona mentalnih bolesti. Ali magnetni grafenov oksid (MGO) ne može sam poboljšati elektrokemijske signale. S tim u vezi, nakon sinteze MGO-a, IL je uspostavljen na kompozitu. Zatim su nanočestice zlata (AuNP) i molekularno utisnuti polimer (MIP) modificirali MGO nanokompozit. MIP polimerizacija nastavljena je metakrilnom kiselinom (MAA) u prisutnosti dopamina kao modelne molekule. Razvijeni senzor s modificiranim nanokompozitom proučavan je tehnikama ciklične voltametrije (CV) i diferencijalne pulsne voltametrije (DPV). Modificirani senzor na bazi nanokompozita sa širokim linearnim rasponom koncentracije, između 1×10^{-7} do 1×10^{-4} mol L⁻¹ i granicom detekcije od 1×10^{-8} mol L⁻¹ (S/N = 3) korišten je za detekciju dopamina u biološkim uzorcima. Ovi rezultati dokazuju da je MGO poboljšao aktivna mjesta površinskoga nanokompozita, a IL je povećao vodljivost u baziranome elektrokemijskom senzoru za detekciju dopamina.

Ključne riječi:

magnetne nanočestice, grafenov oksid, ionska tekućina, nanočestice zlata

Author's contribution

Farzaneh Shaker (Ph.D. student of Analytical Chemistry): performed experiments, provided the report and wrote the article. **Mohammad Taghi Vardini** (Assistant Professor, Analytical Chemistry): proposed ideas and guided the research. **Moosa Es'haghi** (Assistant Professor, Analytical Chemistry): proposed ideas and guided the research. **Ebrahim Ghorbani Kalhor** (Associate Professor, Analytical Chemistry): proposed ideas and guided the research.